

# REMOVAL OF CRYSTAL VIOLET DYE FROM WASTEWATER USING SYNTHESIZED ACTIVATED CARBON FROM ADANSONIA DIGITATA IN TWO DIFFERENT GEOGRAPHICAL REGIONS OF SATARA DISTRICT

M. S. Deshmukh<sup>1</sup>, T. V. Barge<sup>2</sup>, T. A. Mane<sup>2</sup>, A. S. Jadhav<sup>2</sup>, A. M. Nalawade<sup>2</sup>, P. V. Chavan<sup>1\*</sup>

<sup>1</sup>Department of Chemistry, Yashwantrao Chavan Institute of Science, Satara, Karmaveer Bhaurao Patil University, Satara- 415001, Maharashtra, India.

<sup>2</sup>Department of Chemistry, Lal Bahadur Shastri College of Arts, Commerce & Science, Satara, Shivaji University, Kolhapur- 416004, Maharashtra, India.

Corresponding Author Address: [pvchavanchem@gmail.com](mailto:pvchavanchem@gmail.com)

DOI: <https://doi.org/10.63001/tbs.2025.v20.i01.pp460-469>

## KEYWORDS

Adsorption,  
Activated Carbon (AC),  
Dye Removal,  
Crystal Violet Dye(CVD),  
Adansonia digitata (baobab)  
tree branch.

Received on:

04-01-2025

Accepted on:

02-02-2025

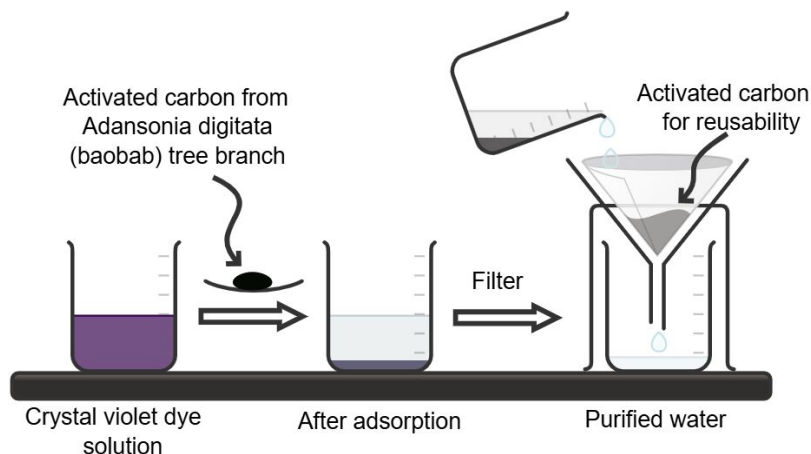
Published on:

28-02-2025

## ABSTRACT

The increasing presence of synthetic dyes, such as crystal violet dye (CVD), in wastewater poses significant environmental, aquatic and health challenges. This study focuses on the synthesis of two types of activated carbon from *Adansonia digitata* (baobab) tree branch which was collected from Dahiwadi, and Menavali in Satara district, a cost-effective and sustainable adsorbent for dye removal. Activated carbon(AC) was produced by chemical activation with potassium hydroxide (KOH) followed by thermal treatment. This Activated Carbon was characterized using scanning electron microscopy (SEM), Fourier-transform infrared spectroscopy (FTIR), and X-ray diffraction (XRD) analysis. Batch adsorption experiments were carried out to assess the impact on essential parameters, including initial dye concentration, pH, adsorbent dosage and contact time. The results demonstrated high adsorption efficiency, with a maximum removal percentage exceeding 99.09% under optimal conditions. This study highlights the potential of *Adansonia digitata* tree branch (ADTB) waste-derived activated carbon as an eco-friendly and efficient solution for treating dye-contaminated water.

## GRAPHICAL ABSTRACT:



## INTRODUCTION

Surface water, which comes from rivers, lakes, canals, and dams is an essential resource that supplies one-third of domestic families' drinking water and three-fourths of the water used for agriculture and industry [1]. We have 70% water on our planet, but only 3% of that water is usable due to various sources, including ice-covered mountains. At least one month of the year, Globally, 2.7 billion people are affected by shortages of water and approximately 1.1 billion people lack the ability to clean water[2]. Freshwater pollution has increased and clean water resources have suffered as a result of homes and businesses releasing wastewater into the environment[3]. Because traditional water remediation techniques are expensive and challenging to remove from surface water, the amount of micro pollutants per litre of surface water keeps rising. The negligent river fish have been found to contain heavy metals that may be harmful to human health as a result of industrial effluents being released into surface water[4]. The Sustainable Development Goals provide a global framework for cooperation on water and sanitation issues. There are seventeen goals altogether. Sustainable Development Goal No. 6, "Clean Water & Sanitation," aims to provide clean water to all people within the next 15 years, and proper hygiene and sanitation on a worldwide basis[5]. yearly, tonnes of wastewater are released into the environment from various industrial sources, including plastics[6], leather[7], cosmetics[8] and most important is printing, textiles and dye manufacturing industries[9-10]. Aquatic life in the receiving environment is at risk when even a tiny quantity of dye is present in the water because it lowers the concentration of dissolved oxygen and the water's clarity. For many years, there has been evidence of air pollution and the negative environmental impacts of industrial operations[11].

Production of high-quality AC is necessary economically due to the growing demand for this effective and affordable method of treating environmental pollution. If cost-effective production techniques and inexpensive precursor materials are used, it is possible[12]. Activated carbon is used in many water treatment applications because it is known to be a highly absorbent matter[13]. A wide variety of plants, including bamboo, plant leaves, corncobs, almond, coconut, peanut, and rice husk shells, as well as wood, sawdust, pine wood, orange peel, and other biological wastes, have been used as raw materials to make AC[14-15]. Carbonaceous material is transformed into a truly porous material with a large surface area available for component separation or adsorption through physical and chemical processes to create AC. The surface area of 1 g of AC has been calculated to be larger than 3000 m<sup>2</sup>[16]. Activated carbon's price is one of the main barriers to applying this adaptable substance in pollution reduction applications like water and wastewater treatment[17]. In comparison to conventional methods, AC made from biomass has emerged as one of the most promising alternatives due to its cost-effectiveness and environmentally friendly aspect. The high adsorption capacity, affordability, and sustainability of AC derived from biomass make it a desirable option for water treatment[18]. The two primary types of AC that are utilised in wastewater and water treatment procedures vary in shape and size. These are AC in powder form (PAC) and granular activated carbon (GAC) [19]. The most popular AC in water treatment methods is GAC. Its typical surface area is 1050 m<sup>2</sup> g<sup>-1</sup>, and its particle sizes range 12 × 40 mesh (0.420 to 1.680 mm)[20].

In 2014, Barricade jagannath[21] demonstrated the trend of annual rainfall by tahsil in Maharashtra State's Satara District from 1991 to 2011. Eastern part of satara district such as Man, Khatav, Khandala, and Phaltan tehsils receive 473 mm of rainfall on average per year, while the western Satara district in Mahabaleshwar, Jawali, and Patan tehsils receive 5000 mm, and the middle and central Satara, Wai, Kardala, and Koregaon tehsils receive 1200 mm. The Satara district's eastern region has historically been the most severely impacted by drought.

In this study, We made activated carbon adsorbents from the *Adansonia digitata* (baobab) tree branch (ADTB) at Dahiwadi and Menavali in Satara, Maharashtra, India for comparative study by using KOH as activated agents. The typical pH of commercial AC is neutral or slightly alkaline in nature. Because AC is commonly used in the water industry to purify water, the water being purified may become acidic or basic if the pH is outside of the neutral range. Nonetheless, The AC produced in this study has a final pH that is within the range of commercially available AC that is 6.8 to 7.2. Using modern surface analysis methods, the physicochemical characteristics of the produced AC were examined. Lastly, the ACs' adsorption ability made from *Adansonia digitata* (baobab) tree branch- Dahiwadi (ACADTB-D) and second sample of AC from *Adansonia digitata* (baobab) tree branch- Menavali(ACADTB-M). The physicochemical properties of the prepared ACs were investigated using modern surface analysis techniques. Finally, the adsorption capacity of the ACs prepared from *Adansonia digitata* tree branch (AC-ADTB) as waste with CVD in water were also investigated.

Since many studies have been done in the past to synthesise high-quality AC, most of them employ typical preparation techniques to synthesise relatively expensive products. The comparative study of dye adsorption onto synthetic AC from *Adansonia digitata* in different geographic regions, which has been shown to be a cost-effective and high-quality AC production method, is not widely reported.

## 2. Materials and methods

### 2.1 Materials & chemicals

Pure chemicals have been used without any additional processing: Crystal violet dye(CVD) (C<sub>25</sub>H<sub>30</sub>ClN<sub>3</sub> 88%, Loba Chemie ) dissolved at a concentration of 100 mg/L in distilled water. Potassium Hydroxide (KOH) 85%, The *Adansonia digitata* (baobab) tree branch (ADTB) were harvested at dahiwadi and menavali in Maharashtra, India.

### 2.2 Preparation of adsorbent and dye solution

*Adansonia digitata* (baobab) tree branch (ADTB) was employed as an activated carbon source in this study, which was obtained from Dahiwadi (ACADTB-D) and Menavali (ACADTB-M) are villages in Satara District. It was harvested between January and March. In order to produce AC, ADTB must be carbonised in an atmosphere with very little airflow in order to remove volatiles and leave behind a porous carbon structure with a large surface area. As seen in fig.1, KOH was applied as a chemical reagent during the activation process. *Adansonia digitata* (baobab) tree branch carbon(ADTB) It was soaked in KOH for 24 hours, filtered, and the chemically loaded ADTB that resulted was put in a furnace for 60 minutes at the highest possible carbonisation temperature of 270°C. The rate of heating was maintained constant throughout all experiments. Following cooling, deionised water was used to repeatedly wash the AC, and it was then dried at 105°C. The carbonised material was used in adsorption experiments after being sieved to a size of 125-250 mm.

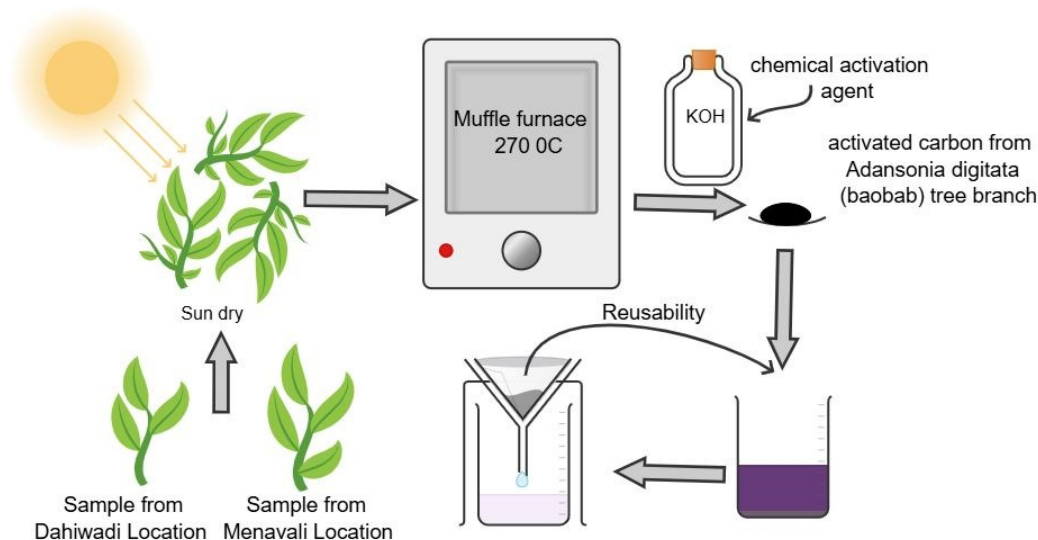


Figure 1. Preparation of Activated Carbon from *Adansonia digitata* (baobab) tree branch which was collected from Dahiwadi, and Menavali in Satara district.

Through a series of experiments, the ACADTB adsorbent's ability to remove crystal violet dye was examined and improved. Initial crystal violet dye (CVD) concentration, initial adsorbent dosage,

and solution pH were among the parameters examined. Typically, 100 mg of the ACADTB adsorbent and 20 millilitres of a CVD aqueous solution with a known starting concentration (1-10 and 20-200 mg/L) were combined to perform batch adsorption studies. In the fig 2 Show 2D structure of Crystal Violet dye.

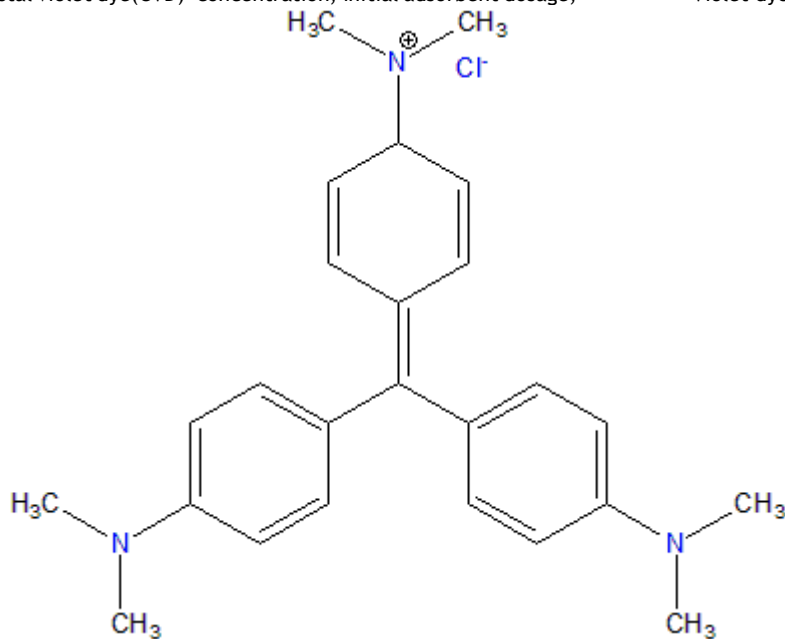


Figure 2. 2D structure of Crystal Violet dye.

### 2.3 Batch adsorption experiments

The mixture of dye and adsorbent solution was stirred and then filtered. By passing the supernatant solution through filter media and then placing the filtrate to UV-vis analysis (UV-1800 spectrometer) at 590 nm, the amount of CVD that persisted in the supernatant at different times was measured. The pH of the CVD solution was raised from 2 to 12 in the pH experiment making 0.1 M NaOH and 0.1 M HCl. Experiments to determine the batch adsorption kinetics were conducted using an adsorbent dosage of 10 mg and 10 ml of CVD (60 mg L<sup>-1</sup>) at pH 4.0 at various time intervals in order to evaluate the impact of the contact time on the CVD adsorption.

#### 2.3.1 Effect of initial CVD concentration

In ten 100 ml conical flasks, adsorption experiments were carried out with AC-ADTB as an adsorbent and CVD as an adsorbate. 100 mg of AC were present in 50 ml of crystal violet solutions in each flask, with initial concentrations varying from 1 mg/L to 10 mg/L. An Orbital shaker BTI-05 was used to shake the set of flasks at 180

rpm and 25 °C. For fifteen minutes, shaking persisted in order to give the system time to reach equilibrium. Following the achievement of equilibrium, the samples were run through Whatman filter paper and measured for crystal violet concentrations in the solution using a UV spectrophotometer (UV-1800) set to 590 nm. Calibration curves were obtained using crystal violet standard solutions ranging from 10 to 200 mg/L.

#### 2.3.2 Effect of AC-ADTB dosage

Initially, the adsorption experiment was conducted without an adsorbent in order to measure the adsorption of crystal violet dye onto glass bottles. It was observed that no adsorption took place during the experiment. There are financial advantages to being able to remove significant amounts of toxic substances from water using a small amount of adsorbent. Thus, adsorbent dosages ranging from 10 to 200 mg were employed to ascertain the impact of various concentrations of ACADTB-D and ACADTB-M on removal of crystal violet. A high adsorbent dosage causes the adsorption sites on the AC to overlap, which is why the higher the adsorbent

dosage, the less crystal violet was adsorbed at equilibrium.. However, as the adsorbent dosage was increased, the crystal violet adsorption efficiency increased between 60 and 70 mg before plateauing at higher concentrations 60 mg was used in later experiments as the dosage of adsorbent.

#### 2.4 Characterization techniques

The morphology and structure of the pores during the activation of the carbon surface from *Adansonia digitata* (baobab) tree branch were characterised and examined with a JEOL JSM-IT200 scanning electron microscope (SEM). Additionally, the elemental content by using Energy Dispersive X-ray Spectroscopy (EDX, Rigaku Miniflex 600), the adsorbent surface was identified., and by using Fourier transform infrared (JASCO FT/IR-4600 typeA) analysis, the functional groups of the adsorbent surface have been studied over the 400-4000  $\text{cm}^{-1}$  wavenumber range.

##### 2.4.1 Scanning electron microscopy (SEM)

An SEM technique (Model JEOL JSM-IT200) was used to study the physical characteristics, morphology and distribution size of adsorbents.

##### 2.4.2 X-ray diffraction (XRD)

### 3. Result and Discussion

#### 3.1. Characterization

##### 3.1.1 Scanning electron microscopy (SEM) Analysis

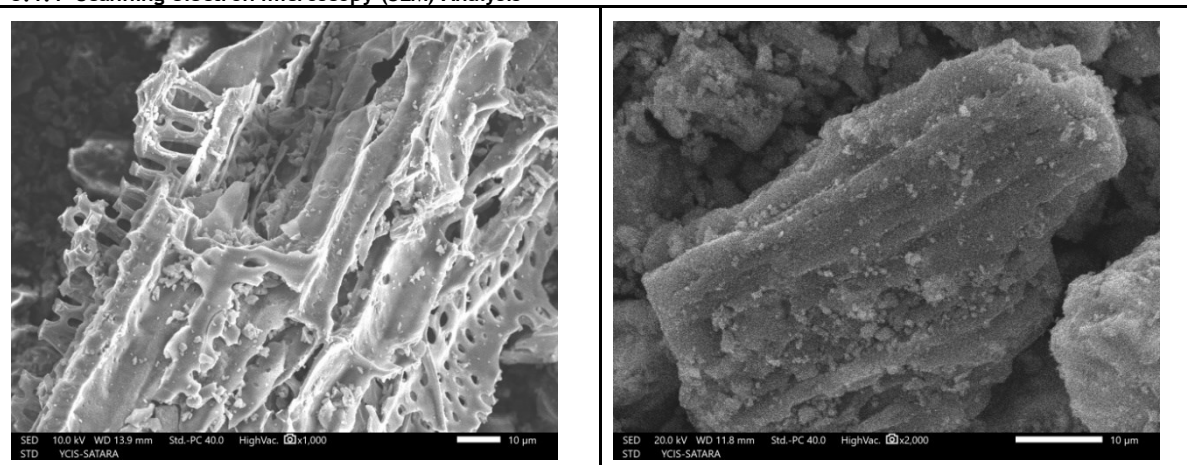


Figure 3. Scanning electron microscopy (SEM) micrographs of sample [A] ACADTB-D and sample [B] ACADTB-M

The SEM pictures of the AC made from the branch of the *Adansoniadigitata* (baobab) tree are displayed in Figure 3. The AC materials made from the branches of *Adansonia digitata* (baobab) trees using the chemical agent KOH were demonstrated in the results. The absolute best SEM sample image of AC [A] According to the ACADTB-D results, numerous microscopic pores developed on the material's surface. Comparable to other authors' studies on AC. This outcome is the result of the activating agent KOH affecting the material's deep surface and the ideal activation conditions being determined. In image [B], ACADTB-D appears to have a more porous structure than ACADTB-M. As expected, the surface The ACADTB-D's area is greater than the ACADTB-M's.

Bragg's law and X-ray diffraction analysis were used to determine the powdered AC and crystal structure. The machine model was the Rigaku Miniflex 600, India, and it had a copper lamp that ran at 40 kV. The analysis was conducted using the two theta range of 7 to 80, and the scanning speed was set at 0.05 degrees per second.

##### 2.4.3 Fourier-transform infrared spectroscopy (FTIR)

In order to study the interaction of the surface functional groups of adsorbents, infrared studies were carried out. The samples' IR adsorption range was calculated by Model Name FT/IR- 4600 type A (India) with the range Start 399.193  $\text{cm}^{-1}$  and End 7800.65  $\text{cm}^{-1}$

##### 2.4.4 Energy dispersive X-ray (EDX) analysis

One method for examining a material's structure to ascertain its purity and percentage distribution of chemical elements is the energy dispersive X-ray (EDX) technique. SED signal, 10.0 kV landing voltage, 14.0 mm WD, x500 magnification, and vacuum mode Before the adsorption process, a high vacuum connected to a SEM was used to examine whether carbon and oxygen elements were present in the adsorbents and how they were distributed at the material surface.

##### 3.1.2 EDX study of activated carbon from *Adansonia digitata* (baobab) tree branch adsorbent

The use of Energy Dispersive X-ray Spectroscopy (EDX) analysis, the element as shown in fig.4 compositions and observing the morphological concepts of sample surfaces. Ultra-thin element light windows on an EDX detector allow it to identify elements with atomic numbers greater than 4[26]. The EDX technique was used as well in the contamination analysis because the presence of particular substances can impact certain issues, like the content's quality [27]. Table 1's EDX spectrum results indicate the existence of C and O elemental contents (weight percentages) are 60.60 and 39.40 percent, respectively.



Table 1. The presence of elemental contents of C and O

[A]

IR spectrum of compound 1a. The x-axis represents Wavenumber [cm<sup>-1</sup>] from 4000 to 400, and the y-axis represents %T from 70 to 100. The spectrum shows characteristic absorption bands for an aldehyde, including a strong C=O stretch at 1694.23 cm<sup>-1</sup> and a C-H stretch at 2927.23 cm<sup>-1</sup>. Other labeled peaks include 3215.72 cm<sup>-1</sup>, 3086.57 cm<sup>-1</sup>, 3062.54 cm<sup>-1</sup>, 3039.54 cm<sup>-1</sup>, 2973.47 cm<sup>-1</sup>, 2957.78 cm<sup>-1</sup>, 2940.83 cm<sup>-1</sup>, 2927.47 cm<sup>-1</sup>, 2914.97 cm<sup>-1</sup>, 2898.43 cm<sup>-1</sup>, 2886.26 cm<sup>-1</sup>, 2348.85 cm<sup>-1</sup>, 1861.44 cm<sup>-1</sup>, 1619.91 cm<sup>-1</sup>, 1562.06 cm<sup>-1</sup>, 1454.06 cm<sup>-1</sup>, 1392.35 cm<sup>-1</sup>, 1318.11 cm<sup>-1</sup>, 1033.66 cm<sup>-1</sup>, 972.912 cm<sup>-1</sup>, 781.029 cm<sup>-1</sup>, 652.786 cm<sup>-1</sup>, 521.65 cm<sup>-1</sup>, and 442.424 cm<sup>-1</sup>.

[B]

IR spectrum of compound 1b. The x-axis represents Wavenumber [cm<sup>-1</sup>] from 4000 to 400, and the y-axis represents %T from 40 to 100. The spectrum shows characteristic absorption bands for an aldehyde, including a strong C=O stretch at 1694.23 cm<sup>-1</sup> and a C-H stretch at 2927.23 cm<sup>-1</sup>. Other labeled peaks include 3333.36 cm<sup>-1</sup>, 3086.57 cm<sup>-1</sup>, 3062.54 cm<sup>-1</sup>, 3039.54 cm<sup>-1</sup>, 2973.47 cm<sup>-1</sup>, 2957.78 cm<sup>-1</sup>, 2940.83 cm<sup>-1</sup>, 2927.47 cm<sup>-1</sup>, 2914.97 cm<sup>-1</sup>, 2898.43 cm<sup>-1</sup>, 2886.26 cm<sup>-1</sup>, 2348.85 cm<sup>-1</sup>, 1861.44 cm<sup>-1</sup>, 1619.91 cm<sup>-1</sup>, 1562.06 cm<sup>-1</sup>, 1453.1 cm<sup>-1</sup>, 1392.35 cm<sup>-1</sup>, 1319.07 cm<sup>-1</sup>, 1036.55 cm<sup>-1</sup>, 970.983 cm<sup>-1</sup>, 781.029 cm<sup>-1</sup>, 672.071 cm<sup>-1</sup>, 520.686 cm<sup>-1</sup>, and 441.872 cm<sup>-1</sup>.

Fig. 5. FT-IR spectra of activated carbon prepared using sample [A] *Adansonia digitata* (baobab) tree branch- Dahiwadi (ACADTB-D) and [B] *Adansonia digitata* (baobab) tree branch- Menavali(ACADTB-M), Experimental condition: calcination temperature 270 °C

Additionally, the AC's FT-IR spectra from the *Adansonia digitata* (baobab) tree branch-Dahiwadi (ACADTB-D) are displayed in Figure 5[A]. These spectra indicate that the ACs contain numerous functional groups and that there are many functional groups in the AC that correlate to different oscillating wavelengths, including one that is 3562.84  $\text{cm}^{-1}$ . The wavelengths at 1318.11  $\text{cm}^{-1}$  provide the carboxyl functional groups  $\text{C} = \text{O}$ . At the wavelength of 781.029  $\text{cm}^{-1}$ , some oscillations that are characteristic of the aromatic hydrogen (C-H) bonding can be observed. At 652.786  $\text{cm}^{-1}$ , this wavelength is typical for the S-O group (complex  $\text{SO}_2$ ). The wavelength at 1033.66  $\text{cm}^{-1}$  indicates the vibration of the C-N groups in aliphatic amines, alcohol, or phenol[22]. The oscillating peaks at 972.912  $\text{cm}^{-1}$  represent the C-H bond (aromatic hydrogen)[23]. The peaks that fluctuate at a wavelength of 1562.06  $\text{cm}^{-1}$  are indicative of the carboxyl functional groups ( $\text{C} = \text{O}$ ) found in polyphenols [24]. At wavelengths of 3562.84  $\text{cm}^{-1}$  and 3590.81  $\text{cm}^{-1}$ , the peaks for

crystal oscillation-OH (hydrate) and group-OH (hydroxyl) are visible correspondingly [25].

The AC from *Adansonia digitata* (baobab) tree branch-Menavali (ACADTB-M) has a lot of specific functional groups that correspond to a lot of oscillating wavelengths, according to the FT-IR Fig. 5[B] diagram analysis. The group-OH (hydroxyl) and crystal oscillation-OH (hydrate) peaks are located at wavelengths of 3333.36  $\text{cm}^{-1}$  and 3561.88  $\text{cm}^{-1}$ , respectively [25]. The peaks that vary at a wavelength of 1619.91  $\text{cm}^{-1}$  are indicative of the carboxyl functional groups ( $\text{C} = \text{O}$ ) [24]. The wavelength at 1036.55  $\text{cm}^{-1}$  indicates the vibration of the C-N groups in aliphatic amines, alcohol, and phenol [22]. The C-H The oscillating peaks at 970.983  $\text{cm}^{-1}$  represent the bond (aromatic hydrogen) [23].

### 3.1.4. XRD analysis

The AC's XRD spectrum in Figure 6 shows the diffraction peaks that formed on the ACADTB-D and ACADTB-M samples several significant diffraction peaks.

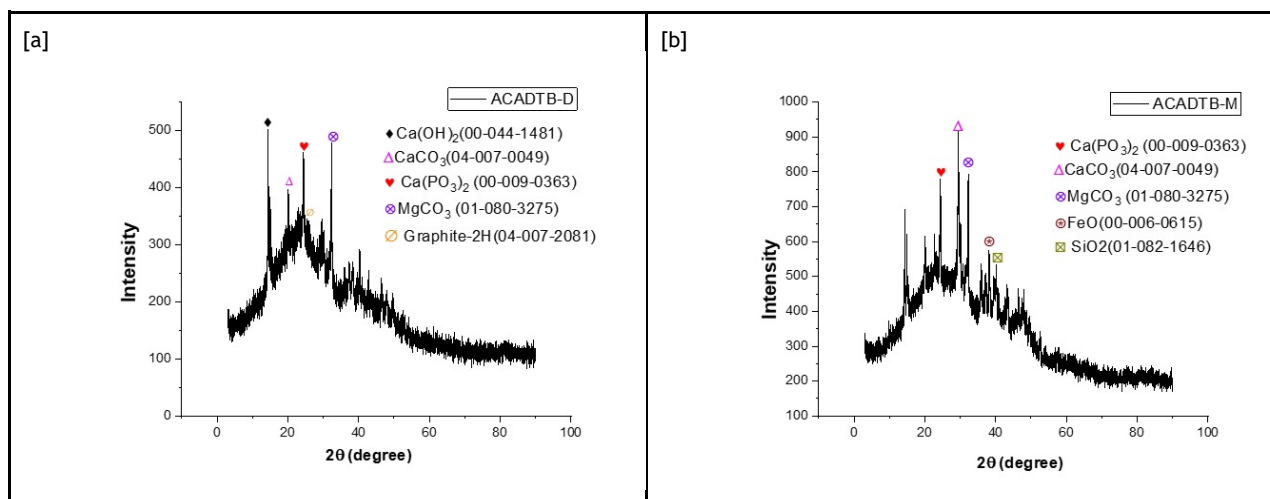


Figure 6. XRD of the prepared sample [a] ACADTB-D and sample [b]ACADTB-M

### 3.2. Effect of initial concentration

The percentage of CVD removed increased and then declined suggesting that the removal of CVD depended on its initial concentration, while the amount of CVD adsorbed increased with

the initial concentration. To describe how the concentration affects Figure 7 illustrates the range of initial CVD concentrations from 1 to 10  $\text{mg L}^{-1}$  that were examined in order to determine the adsorption capacity of the ACADTB-D and ACADTB-M.

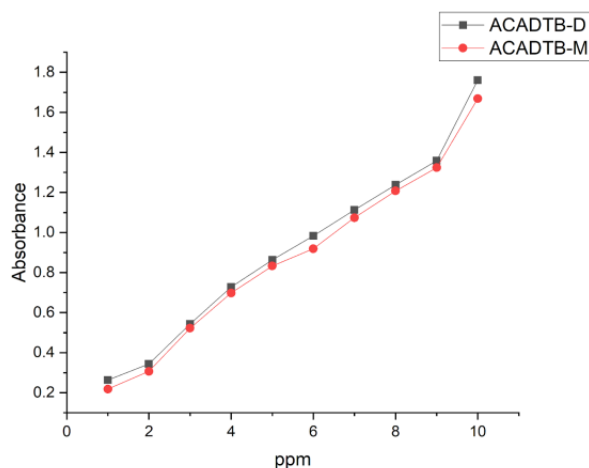


Figure 7. Effects of initial CVD concentration on adsorption capacity of sample ACADTB-D and sample ACADTB-M.

### 3.3. Effect of pH

The pH of the CVD solution had an impact on the surface charge and level of ionisation of the AC and dissociation of the functional groups[28]. A study was carried out to investigate the effects of solution pH on CVD removal and the findings are shown in Fig.8[A] The pH range in which the batch experiment was carried out was 2-12. According to the results, the adsorption efficiency significantly increased and peaked at 95.7% in the pH range of 3-

4, as illustrated by the amount of CVD removal (percentage) in Fig.8[B] But after a pH of 9, the adsorption efficiency sharply declined. The potential changing as the pH changed explains why the amount of CVD removal increased with pH, indicating that the ADTB's surface had a higher positive charge. As a result, the removal percentage increased slightly from 3 to 5 pH and nearly reached 95.7%.

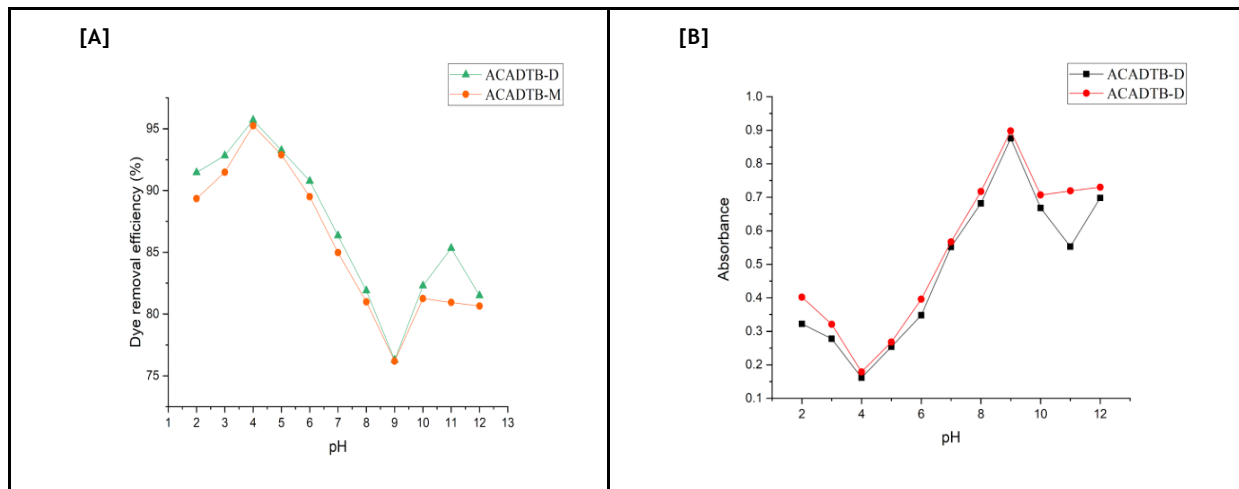


Figure 8. Effect of pH on[A] removal of CVD by ACADTB-D and ACADTB-M. [B] amount of CVD removal (percentage)

### 3.4. Effect of adsorbent amount:

Initially, In order to measure, the adsorption experiment was conducted without an adsorbent. the adsorption of crystal violet dye onto glass bottles. It was observed that no adsorption occurs during the experiment. Economic advantages result from the ability to remove significant amounts of hazardous substances from water using a small amount of adsorbent. Therefore, adsorbent dosages ranging from 10 to 200 mg were applied to determine how different AC concentrations affected the elimination of crystal violet dye. Applying an equation (1),

$$qt = (C_o - C_t)V / m \quad \dots(1)$$

$$\% \text{ Removal} = \frac{(C_o - C_t)}{C_o} \times 100 \quad \dots(2)$$

where V is the volume of the CVD solution (L), m is the mass of the AC adsorbent (g), and  $C_o$  and  $C_t$  are the concentrations of

crystal violet dye at the beginning and time t( $\text{mg L}^{-1}$ ), respectively. Conversely, using equation (1) and substituting  $C_e$  for  $C_t$ , the CVD equilibrium concentration ( $\text{mg L}^{-1}$ ), the amount of CVD adsorbed at equilibrium ( $q_e$ ) is determined. Fig. 9 shows the calculated amount of CVD adsorbed at equilibrium ( $q_e$ ) at each concentration. At high adsorbent dosages, the AC's adsorption sites overlap, so the quantity of As the adsorbent dosage rose, the amount of CVD adsorbed at equilibrium decreased.

To find out how different concentrations of ACADTB-D and ACADTB-M affected the removal of CVD, adsorbent dosages ranging from 10 to 200 mg were used. But when the adsorbent dosage was raised to between 60 and 70 mg, the CVD adsorption efficiency increased as well, plateauing at higher concentrations. This might be explained by The high number of adsorption-active sites and their large surface area[29]. In subsequent studies, 60 mg of ACADTB-D was utilized as the adsorbent dosage because this amount reached the drug's adsorption equilibrium above that level.

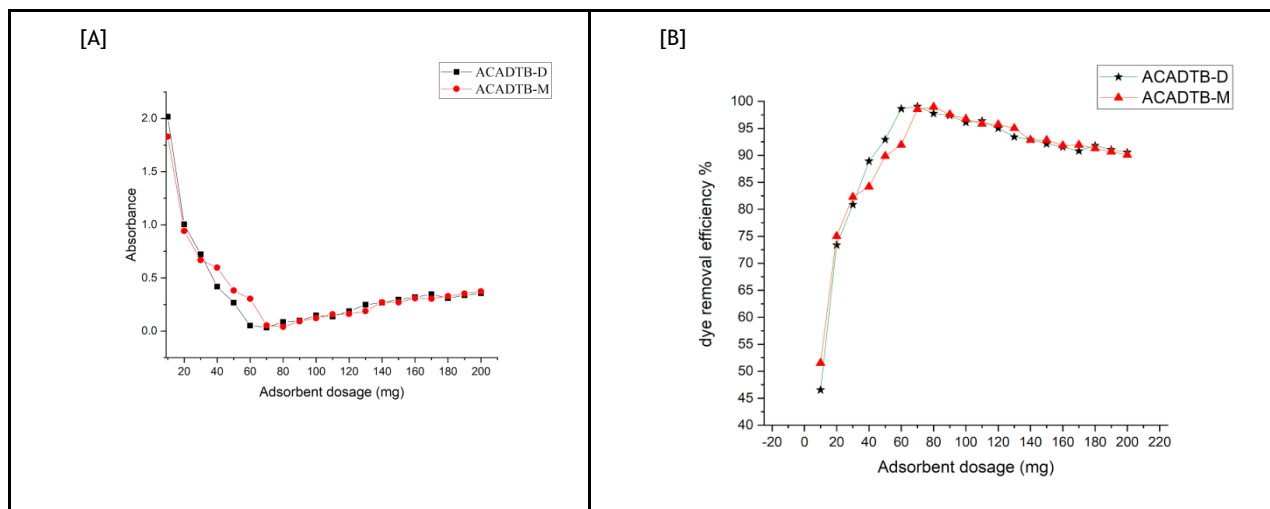




Figure 9. Effects of dosage of ACADTB-D and ACADTB-M on [A] adsorption capacity and [B] adsorption efficiency for removal of CVD.

### 3.5. Effect of the contact period

ACADTB-D appears to have a higher density of accessible active sites or a more favorable pore structure. This facilitates quicker diffusion and binding of dye molecules to its surface, allowing most of the dye to be captured within 7 minutes. In contrast, ACADTB-M structure may present fewer or less accessible active

sites, meaning the dye takes a bit longer around 9 minutes to reach complete adsorption. As shown in Fig. In essence, the removal of dye in 7 minutes with ACADTB-D versus 9 minutes with ACADTB-M. Also The Figure 11 illustrates the dye solution at various time intervals, highlighting the progressive changes in concentration due to adsorption.

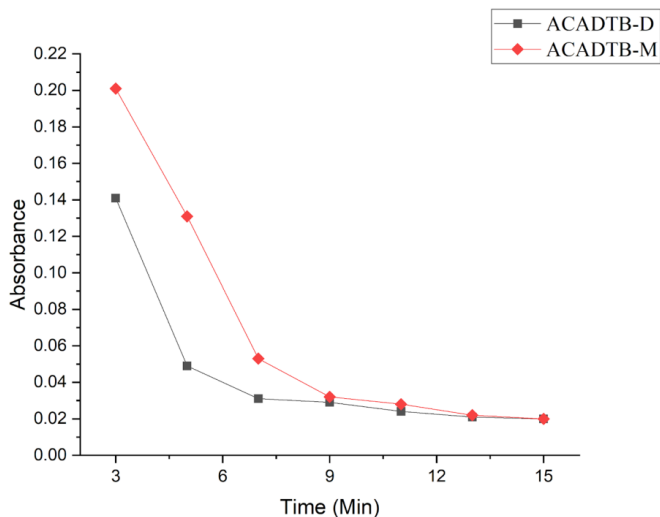


Figure 10. Effect of adsorption time on CVD adsorbed

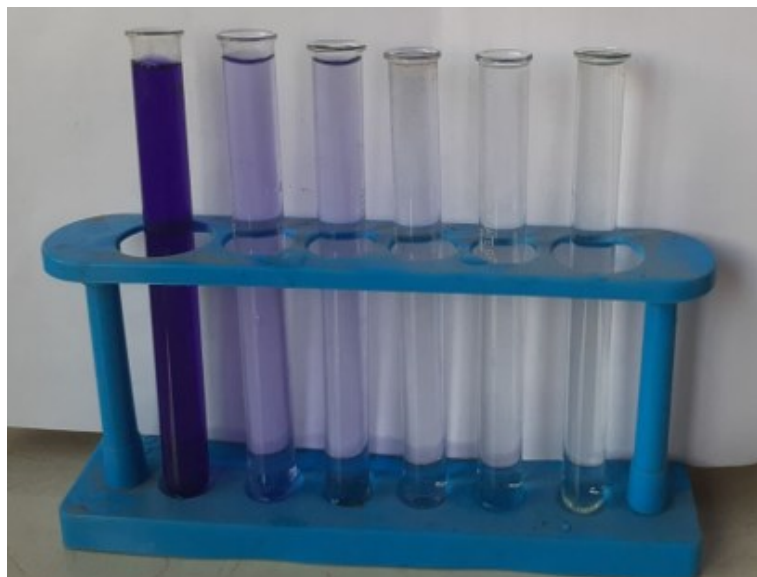


Figure 11. CVD solution at various time intervals

### 3.6 Reusability of ADTB :

The reusability of the ADTB has been determined by examining the removal procedure for six cycles, as illustrated in Fig.12, in order to show the viability of real-world applications. For cycles 1, 2, 3, 4, 5, and 6, the nanocomposite shown removal efficiencies

of 99.09, 98.08, 98.3, 97.7, 97.2, and 96.9%, respectively. Between cycles, there was a small go in the adsorption performance, suggesting that the magnetic nanocomposite could adsorb with high effectiveness. CVD from wastewater, which can subsequently be readily recycled and utilized again.



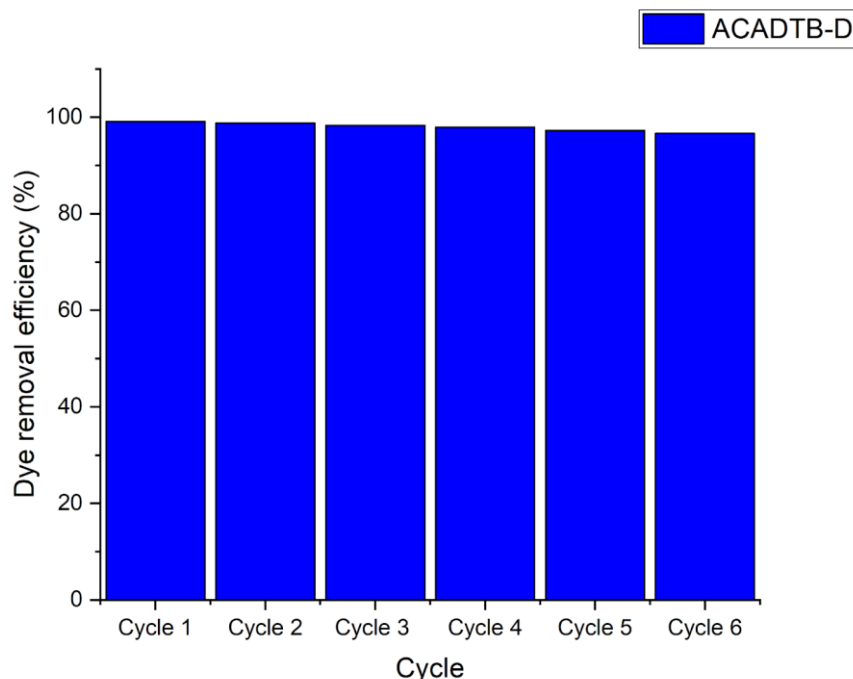


Figure 12. Reusability of ACADTB-D for removing CVD from wastewater

## CONCLUSION

This study investigated the effectiveness of synthetic AC made from baobab (*Adansonia digitata*) in removing crystal violet dye from aqueous solutions, comparing samples from two different geographical regions of Satara District. The results demonstrated that both ACs exhibited significant adsorption capacities, influenced by factors such as surface area, pore design, and the carbon's physicochemical characteristics. Differences in adsorption capacities between the two geographical regions were attributed to variations in the local soil composition, climate, and growth conditions affecting the precursor material. Overall, the study highlights the potential of *Adansonia digitata*-derived AC as a safe and efficient adsorbent for the removal of CVD. Future research should focus on optimizing activation conditions, exploring more regeneration possibilities, and assessing different industrial wastewater applications to enhance its practical applicability in wastewater treatment.

### Declaration of competing interest

The authors declare that they have no known competing financial interests or personal relationships that could have appeared to influence the work reported in this paper.

### Acknowledgment

The authors acknowledge the Department of Chemistry, Yashwantrao Chavan Institute of Science, Satara, the Department of Chemistry, Lal Bahadur Shastri College of Arts, Science and Commerce, Satara, Maharashtra and the Karmaveer Bhaurao Patil University and Shivaji University, Kolhapur, for providing laboratory facilities.

### Data availability

Data will be made available on request.

## REFERENCES

- [1] Chakraborty, S. K., & Chakraborty, S. K. (2021). Geo-hydrological perspectives of riverine flows. *Riverine Ecology Volume 1: Eco-functionality of the Physical Environment of Rivers*, 375-476.
- [2] Kumar, R. (2019). Emerging challenges of water scarcity in India: the way ahead. *International Journal of Innovative Studies in Sociology and Humanities*, 4(4), 6-28.
- [3] Andersson, M., Beale, S. B., Espinoza, M., Wu, Z., & Lehnert, W. (2016). A review of cell- scale multiphase flow modeling, including water management, in polymer electrolyte fuel cells. *Applied Energy*, 180, 757-778.
- [4] Maurya, P. K., Malik, D. S., Yadav, K. K., Kumar, A., Kumar, S., & Kamyab, H. (2019). Bioaccumulation and potential sources of heavy metal contamination in fish species in River Ganga basin: Possible human health risks evaluation. *Toxicology reports*, 6, 472-481.
- [5] Mansell, P., Philbin, S. P., & Konstantinou, E. (2019, September). Infrastructure projects' impact on sustainable development-Case study of a water-utility company. In *Otmc Conference*.
- [6] Altass, H. M., Morad, M., Khder, A. E. R. S., Mannaa, M. A., Jassas, R. S., Alsimaree, A. A., & Salama, R. S. (2021). Enhanced catalytic activity for CO oxidation by highly active Pd nanoparticles supported on reduced graphene oxide/copper metal organic framework. *Journal of the Taiwan Institute of Chemical Engineers*, 128, 194-208.
- [7] Nath, A., Shah, A., Singh, L. R., & Mahato, M. (2021). Waste plastic-derived NiO-MWCNT composite as visible light photocatalyst for degradation of methylene blue dye. *Nanotechnology for Environmental Engineering*, 6, 1-14.
- [8] Jain, H., Yadav, V., Rajput, V. D., Minkina, T., Agarwal, S., & Garg, M. C. (2022). An eco-sustainable green approach for biosorption of methylene blue dye from textile industry wastewater by sugarcane bagasse, peanut hull, and orange peel: A comparative study through response surface methodology, isotherms, kinetic, and thermodynamics. *Water, Air, & Soil Pollution*, 233(6), 187.
- [9] Altass, H. M., Morad, M., Khder, A. E. R. S., Mannaa, M. A., Jassas, R. S., Alsimaree, A. A., & Salama, R. S. (2021). Enhanced catalytic activity for CO oxidation by highly active Pd nanoparticles supported on reduced graphene oxide/copper metal organic framework. *Journal of the Taiwan Institute of Chemical Engineers*, 128, 194-208.
- [10] Malatji, N., Makhado, E., Modibane, K. D., Ramohlola, K. E., Maponya, T. C., Monama, G. R., & Hato, M. J. (2021). Removal of methylene blue from wastewater using hydrogel nanocomposites: A review.

- [11] Zamel, D., & Khan, A. U. (2021). Bacterial immobilization on cellulose acetate based nanofibers for methylene blue removal from wastewater: Mini-review. *Inorganic Chemistry Communications*, 131, 108766.
- [12] Saleem, M. (2024). Sustainable production of activated carbon from indigenous Acacia etbaica tree branches employing microwave induced and low temperature activation. *Heliyon*, 10(2).
- [13] Mouni, L., Belkhiri, L., Bollinger, J. C., Bouzaza, A., Assadi, A., Tirri, A., ... & Remini, H. (2018). Removal of Methylene Blue from aqueous solutions by adsorption on Kaolin: Kinetic and equilibrium studies. *Applied Clay Science*, 153, 38-45.
- [14] Yang, H. M., Zhang, D. H., Chen, Y., Ran, M. J., & Gu, J. C. (2017, June). Study on the application of KOH to produce activated carbon to realize the utilization of distiller's grains. In *IOP Conference Series: Earth and Environmental Science* (Vol. 69, No. 1, p. 012051). IOP Publishing.
- [15] Sabir, A., Altaf, F., Batool, R., Shafiq, M., Khan, R. U., & Jacob, K. I. (2021). Agricultural waste absorbents for heavy metal removal. *Green adsorbents to remove metals, dyes and boron from polluted water*, 195-228.
- [16] Otowa, T., Nojima, Y., & Miyazaki, T. (1997). Development of KOH activated high surface area carbon and its application to drinking water purification. *Carbon*, 35(9), 1315-1319.
- [17] Tuli, F. J., Hossain, A., Kibria, A. F., Tareq, A. R. M., Mamun, S. M., & Ullah, A. A. (2020). Removal of methylene blue from water by low-cost activated carbon prepared from tea waste: A study of adsorption isotherm and kinetics. *Environmental Nanotechnology, Monitoring & Management*, 14, 100354.
- [18] Ullah, S., Shah, S. S. A., Altaf, M., Hossain, I., El Sayed, M. E., Kallel, M., ... & Nazir, M. A. (2024). Activated carbon derived from biomass for wastewater treatment: Synthesis, application and future challenges. *Journal of Analytical and Applied Pyrolysis*, 106480.
- [19] Bansal, R. C., & Goyal, M. (2005). *Activated carbon adsorption*. CRC press.
- [20] Hung, Y. T., Lo, H. H., Wang, L. K., Taricska, J. R., & Li, K. H. (2005). Granular activated carbon adsorption. In *Physicochemical treatment processes* (pp. 573-633). Totowa, NJ: Humana Press.
- [21] Jagannath, B. (2014). Rainfall trend in drought prone region in eastern part of Satara district of Maharashtra, India. *European Academic Research*, 2(1), 329-340.
- [22] Annadurai, G., Juang, R. S., & Lee, D. J. (2002). Use of cellulose-based wastes for adsorption of dyes from aqueous solutions. *Journal of hazardous materials*, 92(3), 263-274.
- [23] Deng, H., Yang, L., Tao, G., & Dai, J. (2009). Preparation and characterization of activated carbon from cotton stalk by microwave assisted chemical activation—application in methylene blue adsorption from aqueous solution. *Journal of hazardous materials*, 166(2-3), 1514-1521.
- [24] Gomez-Serrano, V., Pastor-Villegas, J., Perez-Florindo, A., Duran-Valle, C., & Valenzuela-Calahorra, C. (1996). FT-IR study of rockrose and of char and activated carbon. *Journal of analytical and applied pyrolysis*, 36(1), 71-80.
- [25] Pouretedal, H. R., & Sadegh, N. (2014). Effective removal of amoxicillin, cephalexin, tetracycline and penicillin G from aqueous solutions using activated carbon nanoparticles prepared from vine wood. *Journal of Water Process Engineering*, 1, 64-73.
- [26] Khavryuchenko, V. D., Khavryuchenko, O. V., Shkilnyy, A. I., Stratiichuk, D. A., & Lisnyak, V. V. (2009). Characterization by SEM, TEM and quantum-chemical simulations of the spherical carbon with nitrogen (SCN) active carbon produced by thermal decomposition of poly (vinylpyridine-divinylbenzene) copolymer. *Materials*, 2(3), 1239-1251.
- [27] Sarecka-Hujar, B., Balwierz, R., Ostrozka-Cieslik, A., Dyja, R., Lukowiec, D., & Jankowski, A. (2017, November). Scanning electron microscopy and X-ray energy dispersive spectroscopy-useful tools in the analysis of pharmaceutical products. In *Journal of Physics: Conference Series* (Vol. 931, No. 1, p. 012008). IOP Publishing.
- [28] Crini, G., Peindy, H. N., Gimbert, F., & Robert, C. (2007). Removal of Cl Basic Green 4 (Malachite Green) from aqueous solutions by adsorption using cyclodextrin-based adsorbent: Kinetic and equilibrium studies. *Separation and Purification Technology*, 53(1), 97-110.
- [29] Ghaedi, M., Ghaedi, A. M., Negintaji, E., Ansari, A., Vafaei, A., & Rajabi, M. (2014). Random forest model for removal of bromophenol blue using activated carbon obtained from Astragalus bisulcatus tree. *Journal of Industrial and Engineering Chemistry*, 20(4), 1793-1803.